Journal of Catalysis 263 (2009) 92–97

Contents lists available at ScienceDirect

Journal of Catalysis

www.elsevier.com/locate/jcat

Selective deactivation of gold catalyst

Cristina Della Pina, Ermelinda Falletta, Michele Rossi *, Adriano Sacco [1]

Dipartimento di Chimica Inorganica, Metallorganica e Analitica, Università Degli Studi di Milano, CNR-ISTM, Via Venezian, 21, 20133 Milano, Italy

ARTICLE INFO

Article history:
Received 10 December 2008
Revised 26 January 2009
Accepted 26 January 2009
Available online 11 February 2009

Keywords:
Gold
Catalysis
Poisoning
Molecular model
Oxygen activation
Glucose oxidation

ABSTRACT

The progressive poisoning effect of different molecules on carbon supported gold catalysts has been evaluated during the aerobic oxidation of glucose. A geometrical model has been derived for describing the morphological properties of two catalysts made of carbon supported gold particles having a known size distribution centered at 3.30 and 7.89 nm respectively. The observed deactivation trend follows the order thiocyanate > cyanide ≈ cysteine > thiourea and it obeys an exponential law. The kinetics of catalyst deactivation has been interpreted by considering the important contribute of electronic factors which overlap the space shielding of active sites, due to long range poison–catalyst interaction influencing the entire metal particle. Considering the nature of the molecules showing a high poisoning effect and the promoting effect of OH^-, a molecular model for electronic interactions in gold nanoparticles during the aerobic oxidation of glucose has been proposed where the dioxygen reduction step is differently influenced by soft and hard-nucleophiles.

1. Introduction

Correlation between surface structure and catalytic behavior in solid materials is of strategic importance for producing quick and clean industrial reactions, whereas speculations on the nature of active sites are a matter of scientific relevance for the progress in catalysis [1].

In recent years gold catalysis has received a growing interest [2] due to exciting applications in dihydrogen activation [3], carbon monoxide oxidation [4], synthesis of hydrogen peroxide [5] and selective liquid phase oxidation [6]. Among studies on the mechanistic aspects of gold catalysis [7,8] only a few papers concern morphological aspects of the active sites. In this context, two recent reports are of great relevance because they seem to demonstrate that unsupported gold promotes the low temperature CO oxidation [9] as well as carbohydrates oxidation [10] with an efficiency similar to the supported gold particles. This observation is helpful for simplifying the design of models taking into account only gold species as the active sites.

Considering the liquid phase oxidation of glucose catalyzed by colloidal gold nanoparticles, we observed a very strong dependence of the activity, expressed as *initial rate/total Au concentration*, from the particle size; we call this ratio, represented by T, *turnover number* since it is different from the canonical TOF (*turnover frequency*), *expressed as initial rate/active sites*. In a series of experiments, carried out under the same conditions of temperature, pressure and amount of gold, the turnover number T rapidly decreased during glucose oxidation from a value of 23,000 h^{-1}, for particles having a mean diameter of 3 nm, to zero for particles of about 10 nm [10] (Table 1).

The experimental turnover numbers correlate very well with the diameter d of the particles, expressed in nm, according to the equation:

$$T\ \left(h^{-1}\right) = \left(9{,}22 \cdot d^{-0{,}335} - 4{,}21\right) \times 10^4. \quad (1)$$

This equation, as all the successive others showing the dependence of some experimental variable from another one (in this case T vs d) was obtained by non-linear correlation analysis starting from some arbitrary functions (in this case $T = a \cdot d^b + c$) and searching the values of the constants (a, b, c) with the aid of well known programs, like "Mathematica" or "MathCad." For each correlation we tried several arbitrary functions, in order to optimize the best fit (all the equations so obtained show a correlation coefficient >0.98).

Assuming a simple model of gold nanospheres having the same diameter d, for a constant total amount of gold the external surface S results in inverse proportion to the diameter, $S = k_1/d$, and then if a given reaction rate was simply proportional to the amount of surface atoms we should expect the linear correlation rate $\cdot\, d = k_2$. On the contrary, in the case of glucose oxidation, a strong deviation from the linear dependence of the activity on total surface metal atoms is observed by plotting $T \cdot d$ vs d, where d is the mean diameter of the different catalyst samples (Fig. 1, where the continuous

* Corresponding author.
E-mail addresses: michele.rossi@unimi.it (M. Rossi), adriano_sacco@fastwebnet.it (A. Sacco).
[1] Retired Full Professor.

0021-9517/$ – see front matter
doi:10.1016/j.jcat.2009.01.014

Table 1

d (nm)	T (h^{-1})
2.96	22,836
3.17	19,370
4.33	14,000
4.87	12,065
6.25	9750
7.02	4560
9.92	400

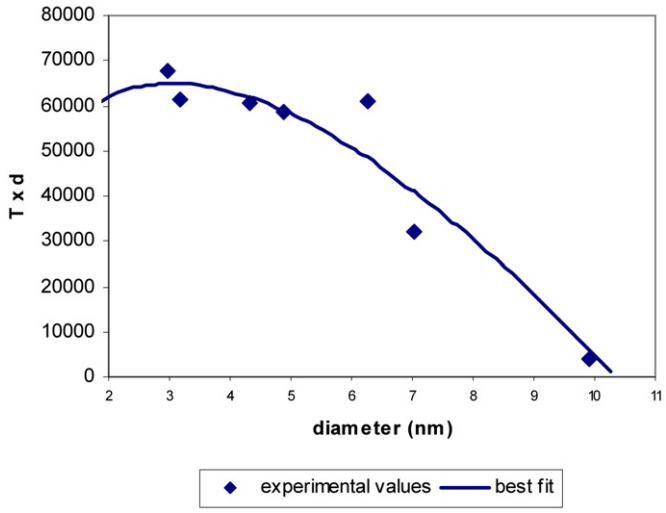

Fig. 1. Deviation from a linear dependence of activity on total surface.

line represents the values of T, obtained from Eq. (1), multiplied by the corresponding values of d).

The high degree of reactivity for gold particles below 5 nm and its rapid decreasing for higher values of the particles size, shown in Fig. 1, have been observed in many experiments of gold catalysis [11–13] and it was interpreted as a coordination effect on the Fermi energy levels, with the subsequent variation of the d-band contribution to the total chemisorption energy of the gold particles [14].

The complexity of heterogeneous catalytic systems is very high because each sample contains a vast number of individual particles characterized by their own peculiar but unknown geometric properties (diameter, structure, conformation of the surface atoms). Moreover, the activity of each site is related both to the dimension of the single particle and the atomic structure of its immediate surroundings, varying from one to another site of the same particle. As a consequence, models are needed for deriving separate information on the contribute of geometrical and electronic factors on the catalytic activity of gold particles having different size. In this work we have investigated a new experimental approach for characterizing the nature of the active sites in differently sized gold particles, which is based on catalyst perturbation induced by poisoning molecules during glucose oxidation.

2. Models

The morphology of gold nanoparticles has been the object of several investigations outlining the appearance of several geometries deriving from different particle dimension and preparation method, which include cubeoctahedra, truncated octahedra, icosahedra, decahedra and amorphous particles [15].

The geometry of "naked" gold particles of diameter larger than 2 nm, formed by nucleation and growth processes in the absence of any support, usually presents structures not too much dissimilar from those of regular polyhedra (mostly cubehoctahedron or truncated octahedron [15–17]), but there are experimental evidences that for the smallest clusters (1–3 nm), Marks decahedron- and icosahedron-structures are quite common [18–20].

In order to derive the geometrical properties of the gold catalyst prepared as colloidal particles, in the absence of experimental high quality HR-TEM images, we have applied either the spherical model or the regular cubeoctahedra/truncated octahedral model.

For the first model the total atoms were calculated from the diameter assuming a close packed fcc structure whereas the surface atoms were calculated assuming a surface packing density intermediate between that of (1 0 0) and (1 1 1) faces. For the polyhedral clusters the diameter and the distribution of atoms (total and surface atoms) could be calculated from the number of atoms on the polyhedron edges [17], but, since we are concerned only with regular polyhedra, we used our simpler equations shown in Appendix A.

In the case of supported particles, the molar fraction of surface atoms available for catalysis was calculated for gold polyhedra laying on an inactive support, like graphite or carbon, with a (111) type face.

Although the particles present in real systems show irregular structures different from perfect spheres or polyhedra, we assume in these models that both the total number of atoms and the related fraction of surface atoms, in a given particle, can be expressed as a continuous function of their diameter (Figs. 2 and 3). It should be outlined that both regular cubeoctahedra and truncated octahedra show a quite similar dependence of the total number of atoms on the diameter. Then the dependence on the particle diameter of the number of the various types of atoms is given by the best fit of the calculated values, as shown by Eqs. (2) and (3), valid in the interval $2 \leqslant d \leqslant 10$ (nm).

$$N_{\text{sphere}} = 30.87 \cdot d^{3},$$

$$N_{\text{polyhedra}} = 13.5 \cdot d^{3,163} - 29, \quad \text{for } 1 \leqslant d \leqslant 7,$$

$$N_{\text{polyhedra}} = 20.64 \cdot d^{2,99} - 550{,}5, \quad \text{for } 6 \leqslant d \leqslant 12, \tag{2}$$

$$\alpha_{\text{sphere}} = \frac{1.31}{d}, \qquad \alpha_{\text{sup ported\_polyhedra}} = 1.107 d^{-0,523} - 0.187, \tag{3}$$

where N represents the total number of gold atom in a particle of diameter d nm, and α represents the ratio [number (or mol) of surface atoms/number (or mol) of gold atoms] in the particle of diameter d nm.

The surface atoms fraction calculated from the mean diameter cannot represent a good measure of the real surface fraction present in the catalytic sample, constituted of a more or less wide particle size distribution. More exactly, in a mixture of particles distributed in i groups according to their diameter, the surface atoms fraction σ_i (included, for each group, in a given interval) can be expressed by Eq. (4):

$$\sigma_i = \frac{\alpha_i \cdot N_i \cdot f_i}{\sum_i (f_i \cdot N_i)}, \tag{4}$$

where f_i is the frequency of the i-group particles, N_i and α_i are respectively the number of atoms and the mean surface atoms fraction of that group of particle. The mean molar ratio (surface atoms/Au) of the catalytic sample is then given by:

$$\sigma = \sum \sigma_i \quad \text{(mol surface atoms/mol Au)}. \tag{5}$$

The meaning of σ must not be confused with that of α: both are expressed as molar ratio, but σ represents the ratio between *all the surface atoms and all the Au atoms present in the sample*, whereas a represents the ratio between *the surface atoms and the Au atoms present in a single particle of a specified diameter*. The value of σ,

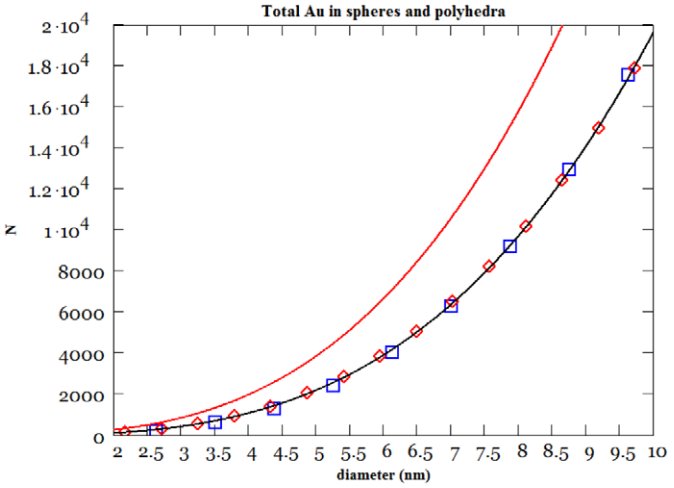

Fig. 2. Total number of Au atoms in spheres and regular polyhedra (red line: spheres; red diamonds: cubeoctahedra; blue box: truncated octahedral; black line: polyhedra best fit). (For interpretation of the references to color in this figure legend, the reader is referred to the web version of this article.)

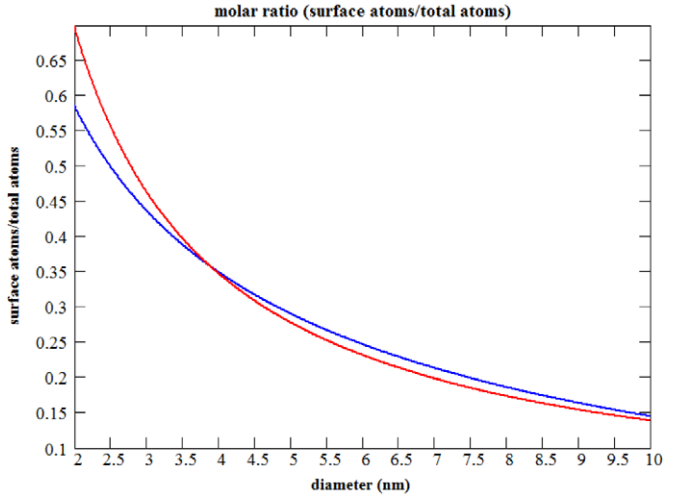

Fig. 3. Molar fraction of surface atoms in regular polyhedra and spheres (red line: dispersion for spherical particles; blue line: dispersion for supported polyhedra). (For interpretation of the references to color in this figure legend, the reader is referred to the web version of this article.)

strongly dependent on the particles frequency in the sample, always differs from that calculated considering the sample constituted of particles of the same mean diameter, that is by assuming σ equals to the value of α shown by particles of that mean diameter.

The estimated mean number N_m of atoms in a single particle becomes:

$$N_m = \sum_i (f_i \cdot N_i) \quad \text{mean number atoms/particle.} \tag{6}$$

Then $1/N_m$ is the estimated molar ratio particles/Au and the mean molar ratio (surface atoms/particle) becomes $\sigma \cdot N_m$.

3. Experimental

3.1. Materials

Gold of 99.999% purity in sponge from Fluka; Carbon support, namely X40S (specific area 1100 $m^2\,g^{-1}$, pore volume 0.37 $ml\,g^{-1}$) from Camel; $NaBH_4$ of purity 96% from Fluka; D-glucose monohydrate (99% pure), δ-gluconolactone (99% pure) from Fluka were used as reagents and reference compounds, without further purification. L-cysteine (>99.5% pure), KCN (>98% pure), KSCN (purity > 99%, thiourea (purity > 99%) from Fluka were used as poisoning compounds, NaOH from Fluka was 99% pure and stored under nitrogen. Gaseous oxygen (SIAD) was 99.9% pure. Milli-Q water obtained by an Academic A-10 Millipore apparatus was used as solvent for all experiments and preparations. $HAuCl_4$ was prepared before the use by dissolving the metal in *aqua regia*. After thermal evaporation of the liquid, the solid was purified by several cycles of dissolution in water followed by evaporation.

3.2. Catalyst preparation and characterization

Two samples of 0.5% Au/C catalyst containing differently sized gold particles were prepared by immobilization of preformed gold sols. In a 150 ml flask, glucose (2.4 g) and 0.3 g of $HAuCl_4$ (10 mg/ml, 3 mg Au) were dissolved in a different amount of water (120 or 30 ml respectively) and treated with $NaBH_4$ (0.8 ml 0.1 M) under vigorous stirring. The resultant colloidal dispersions were immobilized on carbon by adding the support to the solutions under stirring to obtain the theoretical amount of 0.5% of Au. After the adsorption time (20 min) the slurry was filtered and the residual amount of gold (<0.1% total gold) in the mother solution was determined by ICP analysis using a Jobyn Yvon JY24 instrument. The catalysts were filtered and washed with distilled water until the filtrate was chloride free. HR-TEM (LEO 912AB microscope) and XRD (Rigaku D III-MAX horizontal-scan powder diffractometer with Cu$K\alpha$ radiation) analyses were performed to determine the size of the metal crystallites. Two catalysts were finally obtained: Cat-A ($d_m = 3.3$ nm), Cat-B ($d_m = 7.9$ nm). The catalysts were stored in a wet form (ca 20% water).

The mean diameter obtained from the particle size frequency is very similar to that obtained by Scherrer X-ray diffraction method [21] for Cat-A (3.3 nm) and Cat-B (7.9 nm).

3.3. Catalytic oxidation and poisoning tests

Solutions of cysteine, cyanide, thiocyanate, thiourea were prepared by dissolving the proper amount in Milli-Q water, in order to achieve concentrations of 10^{-3}, 10^{-4} and 10^{-5} M. The tests were performed by varying the molar ratio poison/Au in the range 0–0.1. The catalytic test was carried out in a thermostatted (303 K) glass reactor (100 ml) containing 8 g glucose and a fixed amount of catalyst corresponding to 0.5 mg Au. Oxygen was bubbled at atmospheric pressure (1 $NL\,min^{-1}$) through the slurry and the pH was controlled at 9.5 by means of a 751 GPD Titrino (Metrohm) instrument equipped with a titrating solution reserve (NaOH, at proper concentration). NaOH was automatically supplied to maintain the pH of the solution at the desired value and gluconic acid formation versus time was derived from the added amount of the titrating solution. The activity of the original catalyst was derived during the first 200 s; thereafter, an aliquot of the poison at regular intervals of 200 s was added, while the catalytic activity after each addition was considered as the mean T value in the given interval (deviation ±2%).

Adsorption of thiourea on carbon and Cat A catalyst was evaluated in this manner: under the conditions used during the catalytic tests, the aqueous dispersions of 100 mg of the carbon support and 100 mg of Cat-A were separately treated at pH 9.5 both with two different amounts of thiourea (5×10^{-5} mmol and 10^{-3} mmol) under stirring for 5 min. After centrifugation, the residual thiourea was determined in the supernatant solutions by HPLC technique using a Waters 600 E Multisol Vent Delivery System provided with a HP 1050 UV–vis detector and a Supelco C18 25 × 4.6 mm column [22].

4. Results and discussion

By adding small portions of poison (thiourea, cysteine, cyanide or thiocyanate) to the reactants during the oxidation of glucose with O_2 at 295 K and atmospheric pressure in the presence of carbon supported gold catalysts having a different particle size distribution, we followed the decrease of the oxidation rate by the automatic titration of the reaction product gluconic acid. Plotting the values of T/T_0 versus the molar ratio added poison/total Au, different curves for Cat A and Cat B were obtained as shown in Fig. 4 for the four probe molecules.

The gradual addition of the various poisons to the catalyst gives rise to a very rapid decay of the catalytic activity, following very nicely an exponential law of the type:

$$\frac{T}{T_0} = \exp\left(\frac{-a \cdot x}{1 + b \cdot x}\right), \tag{7}$$

where x is the abscissa value and the values of the coefficients a and b, shown in Table 2, depend both on the catalyst particles distribution and the particular poison.

The experimental values of T/T_0 fit very well those calculated by Eq. (7) using the coefficients of Table 2, with a correlation coefficient always greater than 0.99.

For a better comparison of the different poisons it is more reasonable to examine the decay, expressed as function of the fraction of turnover number (T/T_0) vs. the molar ratio (poison/surface atoms) and vs. the molar ratio (poison/particle). These latter ratios can be easily obtained using the values of σ and N_m calculated by Eqs. (4), (5) and (6), since:

$$\frac{\text{poison}}{\text{surface atoms}} = \frac{\text{poison/Au}}{\text{surface atoms/Au}} = \frac{\text{poison/Au}}{\sigma} \tag{8}$$

and

$$\frac{\text{poison}}{\text{particle}} = \frac{\text{poison/Au}}{\text{particle/Au}} = \frac{\text{poison/Au}}{1/N_m}, \tag{9}$$

where the terms "poison," "surface atoms," "Au," "particle" mean the number, or mol, of the respective chemical entities, and $1/N_m$ is the value of the molar ratio (particle/Au).

The size distribution (f) in the particles of Cat-A and Cat-B is shown in Table 3 and the values of σ, N_m and $1/N_m$, obtained by Eqs. (2)–(4) for both catalyst and particle models, are shown in Table 4.

In Fig. 4 the values of T/T_0 are given as a function of the molar ratio (poison/Au) by Eq. (7) with the values of the parameters a and b shown in Table 2. Since Eqs. (8) and (9) show that:

$$(\text{poison/Au}) = \sigma \cdot (\text{poison/surface atoms}) = \frac{1}{N_m} \cdot (\text{poison/particle})$$

the values of T/T_0 can be expressed as a function of molar ratios (poison/surface atoms) or (poison/particles) simply substituting in Eq. (7) the coefficients a and b of Table 2 with those obtained multiplying these values by the suitable values of σ or $1/N_m$ shown in Table 4. As an example, Fig. 5 shows the plots of T/T_0 vs. the molar ratio (poison/surface atom) and (poison/particles) for both the geometric models, using Cat-A and Cat-B poisoned by thiocyanate.

The low amount of reagent able to deeply depress the catalytic activity precludes a simple steric deactivation model. In fact, if each poisoning molecule would be able to suppress only one active site in the catalyst, very high, unrealistic values of the turnover frequency (TOF) would be obtained. Considering Cat-A, whose initial turnover number ($T_0 = 10{,}200\ h^{-1}$) is completely set to zero on adding thiocyanate in the molar ratio $NCS^-/Au = 0.1$, the value of the T_0 becomes:

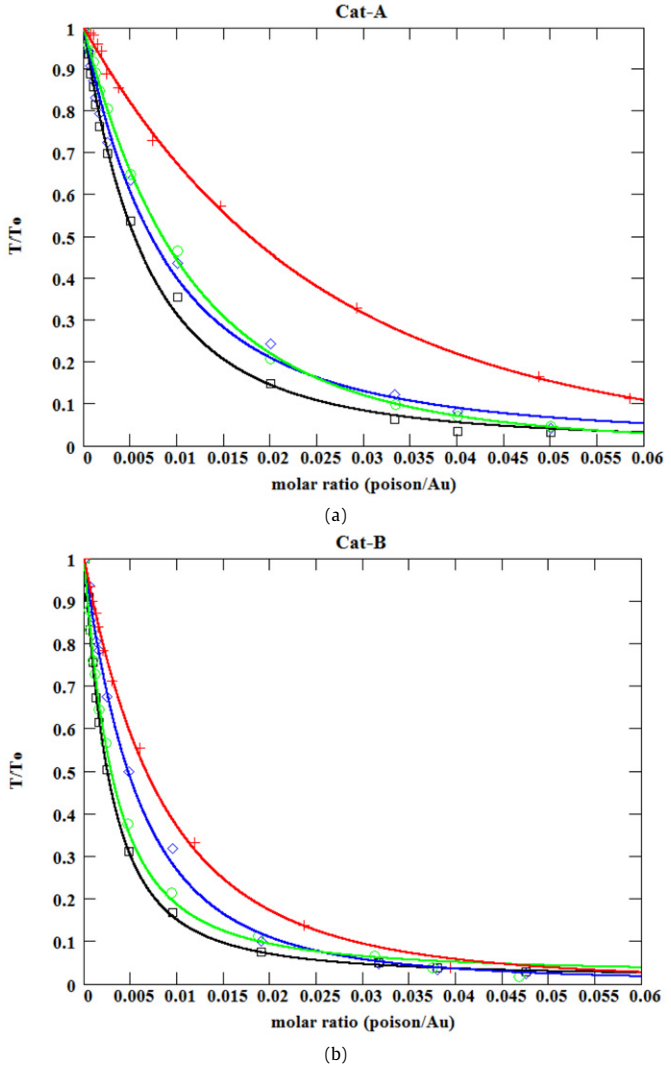

Fig. 4. Residual activity after addition of various amounts of poisoning molecules (red: thiourea; green: cysteine; blue: cyanide; black: thiocyanate; boxes: experimental values; lines: best fit). (For interpretation of the references to color in this figure legend, the reader is referred to the web version of this article.)

Table 2
Values of the coefficients of Eq. (7) for the different poisons (x expressed as molar ratio poison/Au).

Poisoning compounds	Cat-A		Cat-B	
	a	b	a	b
Thiourea	40.0	1.34	115	15.3
Cysteine	88.1	8.30	291	72.9
Cyanide	111	21.0	164	24.1
Thiocyanate	145	25.2	330.5	74.3

Table 3

Cat-A		Cat-B	
d	f	d	f
2–2.5	0.0947	3–4	0.06
2.5–3	0.221	4–5	0.17
3–3.5	0.379	5–6	0.06
3.5–4	0.158	6–7	0.09
4–4.5	0.0842	7–8	0.09
4.5–5	0.0632	8–9	0.17
		9–10	0.11
		10–11	0.1
		11–12	0.09
		12–13	0.06

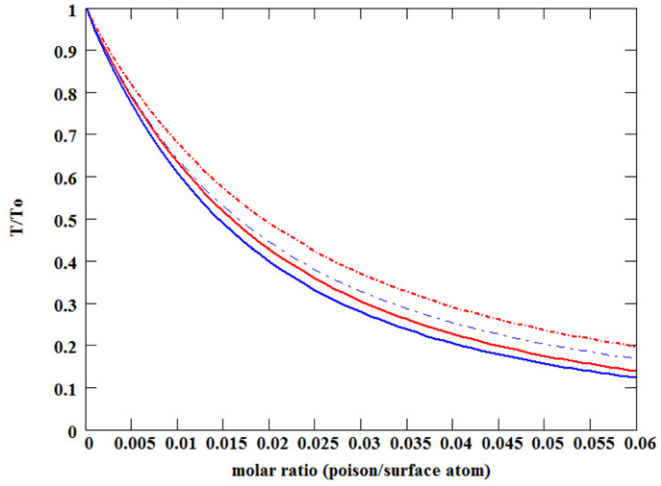

(a)

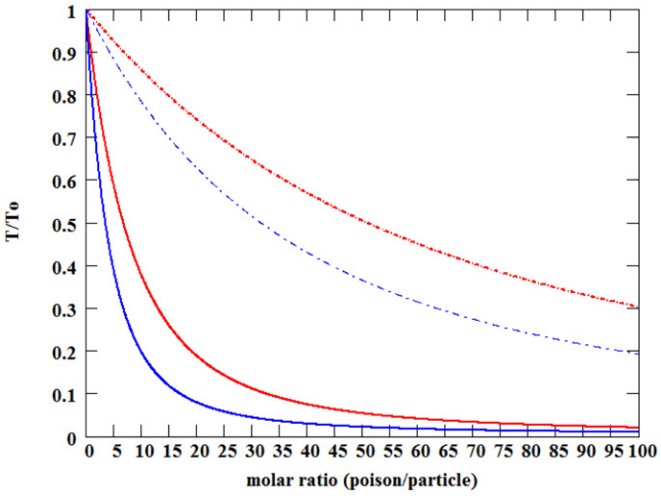

(b)

Fig. 5. Decays of the catalyst activity on thiocyanate addition (Cat-A: lines, Cat-B: points; models: red spheres, blue: polyhedra). (For interpretation of the references to color in this figure legend, the reader is referred to the web version of this article.)

Table 4

	Spheres		Polyhedra	
	Cat-A	Cat-B	Cat-A	Cat-B
σ	0.344	0.129	0.352	0.124
N_m	1242.4	20351.7	641.4	12818.9
$1/N_m$	8.05E–04	4.91E–05	1.56E–03	7.80E–05

$$\mathrm{TOF} = \frac{\text{rate}}{\text{active site}} = \frac{\text{rate/Au}}{\text{active site/Au}} = \frac{T}{\text{active site/Au}} = \frac{T}{\text{poison/Au}} = \frac{10{,}200\ \mathrm{h}^{-1}}{0.1} = 102{,}000\ \mathrm{h}^{-1}.$$

Similarly, still much higher values, even superior to $1.3 \times 10^6\ \mathrm{h}^{-1}$, are obtained considering that the addition of the first aliquots of poison produces a very rapid deactivation: in fact, the addition of thiocyanate to Cat-A in the molar ratio $\mathrm{NCS}^-/\mathrm{Au} = 7.5 \times 10^{-4}$ reduces by 10% the initial value of the turnover number and then the corresponding turnover frequency of the deactivated sites would be:

$$\mathrm{TOF} = 10{,}200 \times 0.10/7.5 \times 10^{-4} = 1{,}36 \times 10^6\ \mathrm{h}^{-1}.$$

It is quite unlikely that these very high values could be due to the deactivation of more sites only by the steric hindrance of a single poisoning molecule since, as it can be seen by applying Eq. (8), the coverage of the particle surface during our experiments is very low. The molar ratio above considered corresponds to the ratio poison/surface atoms $= 7.5 \times 10^{-4}/0.352 = 2.13 \times 10^{-3}$, that is one single poisoning molecule is covering, on average, about 470 surface atoms, and applying Eq. (9) it corresponds to the ratio poison/particle $= 7.5 \times 10^{-4}/1.56 \times 10^{-3} = 0.48$. It is unsustainable that, on average, one single poisoning molecule every 2 gold particles is sufficient to reduce by steric hindrance the turnover number of the catalyst from 10,200 h^{-1} to about 9200 h^{-1}. In conclusion, these data suggest that electronic effects must predominate over the steric ones. It seems likely that the greater effect on small particles is related to the fact that the particles may well starting to lose their metallic character.

The deactivation trend of gold catalysts represented in Figs. 4 and 5 can then be interpreted by assuming that each gold particle behaves as a reactive macromolecule, Au_n, having peculiar electronic properties basically determined by the electron delocalization and, therefore, by the value of n [23].

As experimentally verified, the catalytic performance of each active site decreases by increasing n. Moreover, the binding of deactivating species Y to the particle, to form the modified macromolecule $\mathrm{Au}_n\mathrm{Y}_m$, induces more or less drastic changes of the electronic properties of the original macromolecule, and then of its catalytic activity. As a consequence, the total effect depends on both the values of n and m: as reported in Fig. 5b, the smallest particles of Cat-A are more sensitive to the poisons because the adsorption of a few molecules completely deactivates the catalyst, while the influence is much weaker on the bigger particles of Cat-B. In particular, the adsorption of one single molecule of thiocyanate on a single gold particle causes the 19.6% decrement of the initial activity of Cat-A and only 0.25% of Cat-B considering the polyhedral model or, respectively, 10.8 and 0.016% considering the spherical model. According to a different evaluation, the 50% decrease of the activity of Cat-A is reached on addition of an amount of thiocyanate corresponding to only 1.44% of the total gold surface atoms on the basis of the polyhedral model, and to 1.58% according to the spherical model, as derived from Fig. 5a. In any case, these results can hardly be justified by a simple steric hindrance of more or less active catalytic sites caused by probe molecules.

We should remind that the exponential-like decay of the catalytic activity of gold nanoparticles observed in this work is similar to the kinetics of poisoning of nickel single crystals by sulfur described by Goodman and interpreted by long range electronic effects [24].

The different deactivation power experimentally found for the tested species (thiourea < cysteine ≈ cyanide < thiocyanate) can be in principle due to the following factors: (a) the presence of a dynamic equilibrium between the poison adsorbed on the metallic surface and that left in solution

$$\mathrm{Au}_n\mathrm{Y}_m \leftrightarrow \mathrm{Au}_n\mathrm{Y}_{m-1} + \mathrm{Y}$$

which should produce higher abscissa values in Figs. 4 and 5 for the more dissociated ligand; (b) the electronic modification of the poisoned gold macromolecules, depending on the different nucleophylic properties of the poison.

The hypothesis of point (a) can be excluded on the basis of the following experiment: the weakest poison that we have tested, thiourea, is completely adsorbed (detection limit 5%) on adding this molecule to the gold catalyst, Cat-A, in the molar S/Au ratio 0.02–0.4 with respect to the total gold, that is when thiourea just strongly depresses the original catalytic activity (50–90%). Under identical conditions the carbon support alone is saturated by a small fraction of thiourea (ca. 4% of the lowest employed amount).

Therefore, we consider that the probe molecule bonded to the surface gold produces a change of the electronic density avail-

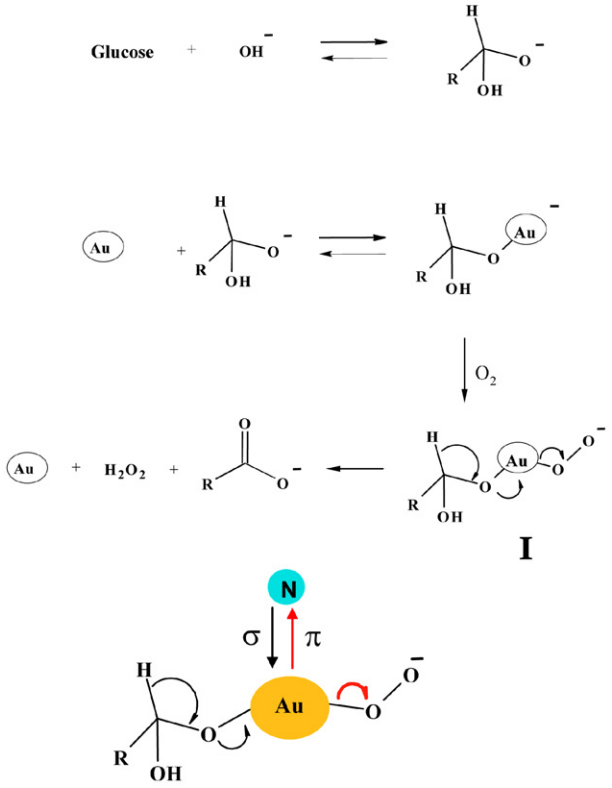

Scheme 1.

able for dioxygen reduction. Considering the general Scheme 1 of glucose oxidation [25], the competition of the poisoning molecule with the reagents can be discussed considering two extreme cases: for a hard nucleophile, no back-donation from metal to the Lewis base is expected, leaving in the reacting solution the original or a higher catalytic effect, as in the case of OH^-. Regarding a nucleophile, N, showing π back-bonding ability, the removal of the electron density from the metal inhibits dioxygen reduction thus decreasing the catalytic property of the entire gold particle.

5. Conclusions

In the present study, the progressive poisoning effect of different molecules on carbon supported gold catalyst has been evaluated during the aerobic oxidation of glucose. It has been proposed that the sharp deactivation is due to the perturbation of the electronic properties of the gold nanoparticles through a long range effect which overlooks the expected subtraction of active sites. In particular, the poisoning effect can be related to the soft character of nucleophilic molecules.

Appendix A. Equations for deriving the number of gold atoms in regular polyhedral fcc-nanoparticles

Symbols

m number of atoms on the polyhedron edge
C number of corners
E number of edges
F_3 number of triangular (1 1 1) faces
F_4 number of square (1 0 0) faces
F_6 number of hexagonal (1 1 1) faces
N_t total number of atoms
N_e total number of atoms inside the edges
N_3 total number of atoms inside the triangular faces
N_4 total number of atoms inside the square faces
N_6 total number of atoms inside the hexagonal faces
N_s total number of atoms on the surface
d diameter (nm) of the polyhedron

Cubeoctahedron

$$C = 12,\ E = 24,\ F_3 = 8,\ F_4 = 6,\ d = 0.54 \cdot m$$

$$N_t = 10 \cdot m^3/3 - 5 \cdot m^2 + 11 \cdot m/3 - 1$$

$$N_e = 12 \cdot (m-2),\ N_4 = 6 \cdot (m-2)^2$$

$$N_3 = 8 \cdot \left[\sum_{n=1}^{m} n - 3 \cdot (m-1) \right]$$

$$N_s = C + N_e + N_4 + N_3$$

Truncated octahedron

$$C = 24,\ E = 36,\ F_6 = 8,\ F_4 = 6,\ d = 0.875 \cdot m$$

$$N_t = 16 \cdot m^3 - 33 \cdot m^2 + 24 \cdot m - 6$$

$$N_e = 36 \cdot (m-2),\ N_4 = 6 \cdot (m-2)^2$$

$$N_6 = 8 \cdot \left[2 \cdot \sum_{n=m-1}^{2m-4} n + (2m-3) \right]$$

$$N_s = C + N_e + N_4 + N_6$$

References

[1] J.M. Thomas, W.J. Thomas, Principles and Practice of Heterogeneous Catalysis, VCH, Weinheim, 1997.
[2] G.C. Bond, C. Louis, D.T. Thompson, Catalysis by Gold, Imperial College Press, Singapore, 2006.
[3] G.C. Bond, P.A. Sermon, G. Webb, D.A. Buchanan, P.B. Wells, J. Chem. Soc. Chem. Commun. 444 (1973).
[4] M. Haruta, T. Kobayashi, H. Sano, N. Yamada, Chem. Lett. 4 (1987) 405.
[5] P. Landon, P.J. Collier, A.J. Papworth, C.J. Kiely, G.J. Hutchings, Chem. Commun. 2058 (2002).
[6] L. Prati, M. Rossi, J. Catal. 176 (1998) 552.
[7] Y. Önal, S. Schimpf, P. Claus, J. Catal. 223 (2004) 122.
[8] P. Beltrame, M. Comotti, C. Della Pina, M. Rossi, Appl. Catal. A 297 (2006) 1.
[9] V. Zielasek, J. Birte, C. Schulz, J. Biener, M.M. Biener, A.V. Hamza, M. Bäumer, Angew. Chem. Int. Ed. 45 (2006) 8241.
[10] M. Comotti, C. Della Pina, R. Matarrese, M. Rossi, Angew. Chem. Int. Ed. 43 (2004) 5812.
[11] (a) J.J. Carberry, J. Catal. 114 (1988) 277;
(b) D. Farin, D. Avnir, J. Catal. 120 (1989) 55;
(c) D. Farin, D. Avnir, J. Am. Chem. Soc. 110 (1988) 2039.
[12] M. Haruta, Catal. Today 36 (1993) 153.
[13] M. Haruta, S. Tsubota, T. Kobayashi, H. Kageyama, M.J. Genet, J. Catal. 144 (1993) 175.
[14] N.S. Phala, E. van Steen, Gold Bull. 40 (2007) 150.
[15] M. Grzelczak, J. Perez-Juste, P. Mulvaney, L.M. Liz-Marzan, Chem. Soc. Rev. (2008) 1783.
[16] K. Page, T. Proffen, H. Terrones, M. Terrones, L. Lee, Y. Yang, S. Stemmer, R. Seshadri, A.K. Cheetham, Chem. Phys. Lett. 393 (2004) 385.
[17] A. Carlsson, A. Puing-Molina, T.V.W. Janssens, J. Phys. Chem. B 110 (2006) 5286, and Supporting information.
[18] H.B. Liù, J.A. Ascencio, M. Perez-Alvarez, M.J. Jacaman, Surf. Sci. 491 (2001) 88.
[19] C.L. Cleveland, U. Landman, T.G. Schaaf, M.N. Schafigullin, Phys. Rev. Lett. 79 (1997) 1873.
[20] J. Turkevich, Gold Bull. 18 (1985) 86.
[21] A.L. Patterson, Phys. Rev. 56 (1939) 972.
[22] J. Rethmeier, G. Neumann, C. Stumpf, A. Rabenstein, C. Vogt, J. Chromatogr. A 934 (2001) 129.
[23] H. Häkkinen, Chem. Soc. Rev. 37 (2008) 1847.
[24] D.W. Goodman, Acc. Chem. Res. 17 (1984) 194.
[25] M. Comotti, C. Della Pina, E. Falletta, M. Rossi, Adv. Synth. Catal. 348 (2006) 313.